

X-ray Testing by Computer Vision

Domingo Mery

Department of Computer Science – Pontificia Universidad Católica de Chile
Av. Vicuña Mackenna 4860(143) – Santiago de Chile

dmery@ing.puc.cl - <http://dmery.ing.puc.cl>

Abstract

X-ray imaging has been developed not only for its use in medical imaging for human beings, but also for materials or objects, where the aim is to analyze –nondestructively– those inner parts that are undetectable to the naked eye. Thus, X-ray testing is used to determine if a test object deviates from a given set of specifications. Typical applications are analysis of food products, screening of baggage, inspection of automotive parts, and quality control of welds. In order to achieve efficient and effective X-ray testing, automated and semi-automated systems are being developed to execute this task. In this paper, we present a general overview of computer vision methodologies that have been used in X-ray testing. In addition, we review some techniques that have been applied in certain relevant applications; and we introduce a public database of X-ray images that can be used for testing and evaluation of image analysis and computer vision algorithms. Finally, we conclude that the following: that there are some areas –like casting inspection– where automated systems are very effective, and other application areas –such as baggage screening– where human inspection is still used; there are certain application areas –like weld and cargo inspections– where the process is semi-automatic; and there is some research in areas –including food analysis– where processes are beginning to be characterized by the use of X-ray imaging.

1. Introduction

Since Röntgen discovered in 1895 that X-rays can be used to identify inner structures, X-rays have been developed not only for their use in *medical imaging* for human beings, but also in *nondestructive testing* (NDT) for materials or objects, where the aim is to analyze (nondestructively) the inner parts that are undetectable to the naked eye. NDT with X-rays, known as *X-ray testing*, is used in many applications such as: analysis of food products, screening of baggage, inspection of automotive parts, quality control of welds, among others. X-ray testing usually involves mea-

surement of specific part features such as integrity or geometric dimensions in order to detect, recognize or evaluate wanted (or unwanted) inner parts.

In order to achieve efficient and effective X-ray testing, automated and semi-automated systems are being developed to execute this difficult, tedious and –sometimes– dangerous task. Compared to manual X-ray testing, automated systems offer the advantages of objectivity and reproducibility for every test. Fundamental disadvantages are, however, the complexity of their configuration, the inflexibility to any change in the evaluation process, and sometimes the inability to analyze intricate images, which is something that people can generally do well. Research and development is, however, ongoing into automated adaptive processes to accommodate modifications.

In this paper, we present the state of the art in X-ray testing using computer vision. We describe a general overview of computer vision methodologies that have been used over the last few years (Section 2). In addition, we review some techniques that have been applied in certain relevant applications using X-ray testing (Section 3). Finally, we introduce a public database of X-ray images that can be used for testing and evaluation of image analysis and computer vision algorithms (Section 4). The paper ends with relevant concluding remarks (Section 5).

2. Principles

In this Section, the principles that govern X-ray testing by computer vision are presented as a general model according to Fig. 1. Applications on X-ray testing –as will be seen in the next Section– follow this general schema. Depending on the way the X-ray images are acquired and analyzed, each block can be (or not be) used.

This Section covers *i*) X-ray image formation, *ii*) single view analysis, *iii*) geometric model and *iv*) multiple view analysis.

2.1. X-ray image formation

X-ray testing is a form of non-destructive testing (NDT) defined as a task that uses X-ray imaging to determine if a

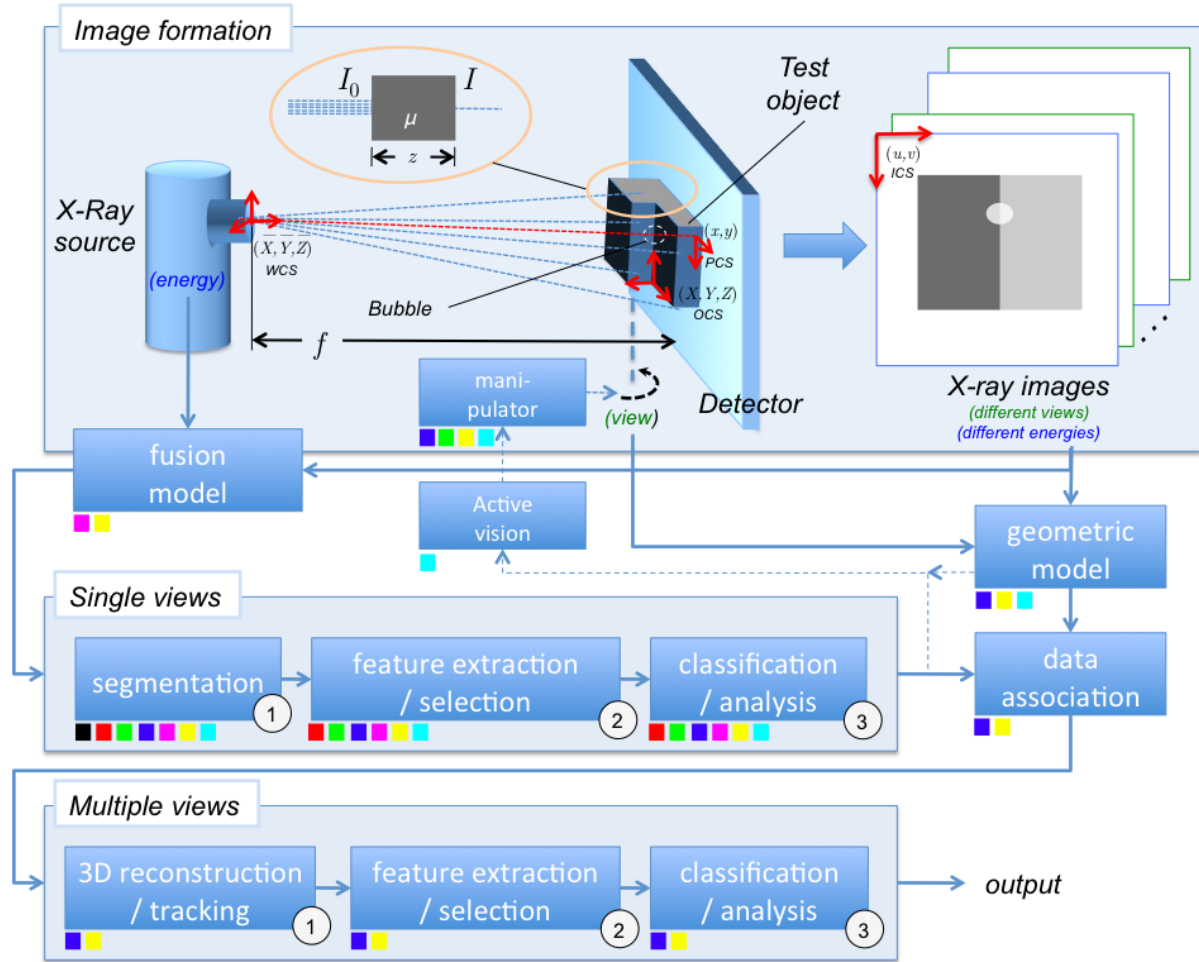


Figure 1. General schema for X-ray testing using computer vision. X-ray images of a test object can be generated at different positions and different energy levels. Depending on the application, each block of this diagram can be (or not be) used. For example, there are applications such as weld inspection that use a segmentation of a single mono energetic X-ray image (black square), sometimes with pattern recognition approaches (red squares); applications like casting inspection that use mono energetic multiple views where the decision is taken analyzing individual views (green squares) or corresponding multiple views (blue squares); applications including baggage screening that use dual-energy of single views (magenta squares) and multiple views (yellow squares); and finally, applications on cargo inspection that employ active vision where a next best view is set according to the information of a single view (cyan squares). In each case, the blocks without the corresponding color square are not used.

test object deviates from a given set of specifications, without changing or altering that object in any way [18]. In X-ray testing, X-ray radiation is passed through the test object, and a *detector* captures an X-ray image corresponding to the radiation intensity attenuated by the object¹. According to the principle of *photoelectric absorption* [2]:

$$I = I_0 \exp(-\mu z), \quad (1)$$

the transmitted intensity I depends on the incident radiation intensity I_0 , the thickness z of the test object, and the energy

¹X-rays can be *absorbed* or *scattered* by the test object. In this paper we will cover only the first interaction. For an interesting application based on the X-ray scattering effect, the reader is referred to [53].

dependent linear attenuation coefficient μ associated with the material, as illustrated in Fig. 1.

The most widely used X-ray imaging systems employed in X-ray testing are digital radiography (DR) and computed tomography (CT) imaging². On the one hand, DR emphasizes high throughput. It uses electronic sensors (instead of traditional radiographic film) to obtain a digital X-ray projection of the target object, for this reason it is simple and quick. A flat amorphous silicon detector can be used as an image sensor in X-ray testing systems. In such detec-

²Computed tomography is beyond the scope of this paper. For NDT applications using CT, the reader is referred to [12].

tors, and using a semi-conductor, energy from the X-ray is converted directly into an electrical signal that can be digitalized into an X-ray digital image [43]. On the other hand, CT imaging provides a cross-section image of the target object so that each object is clearly separated from each other, however, CT imaging requires a considerable number of projections to reconstruct an accurate cross-section image, which is time consuming.

It is worth noting that if X-ray radiation passes through n different materials, with attenuation coefficients μ_i and thickness z_i , for $i = 1, \dots, n$, the transmitted intensity I can be expressed as

$$I = I_0 \exp \left(- \sum_i \mu_i z_i \right). \quad (2)$$

This explains the image generation of regions, that are present inside the test object, as shown in Fig. 1, where a gas bubble is clearly detectable. Nevertheless, X-ray images sometimes contain overlapped objects, making it extremely difficult to distinguish them properly.

Coefficient μ in (1) can be modeled as $\mu = \alpha(Z, E)\rho$, where ρ is the density of the material, and $\alpha(Z, E)$ is the mass attenuation coefficient that depends on the atomic number of the material Z , and the energy E of the X-ray photons. Values for $\alpha(Z, E)$ are already measured and available in several tables (see [19]). In order to identify the material composition –typically for explosives or drug detection– the atomic number Z cannot be estimated using only one image, as a thin material with a high atomic number can have the same absorption as a thick material with a low atomic number [53]. For this purpose, a *dual-energy* system is used, where the object is irradiated with a high energy level E_1 and a low level energy E_2 . In the first case, the absorbed energy depends mainly on the density of the material. In the second case, however, the absorbed energy depends primarily on the effective atomic number and the thickness of the material [49]. Using dual-energy, it is possible to calculate the ratio $R = \ln(I_2/I_0)/\ln(I_1/I_0)$, where I_1 and I_2 are the transmitted intensities I obtained by (1) using energies E_1 and E_2 respectively. Thus, from $R = \alpha(Z, E_2)/\alpha(Z, E_1)$, the term $-\rho z$ is canceled out, Z can be directly found using the known measurements $\alpha(Z, E)$ [17]. From both images, a new image is generated using a *fusion model*, usually a look-up-table that produces pseudo color information [10, 3], as shown in Fig. 2.

2.2. Single view analysis

A computer vision system for single view analysis, as shown in Fig. 1, consists typically of the following steps: an X-ray image of the test object is taken and stored in a computer. The digital image is improved in order to enhance the details. The X-ray image of the parts of interest is found



Figure 2. Generation of a pseudo-color image using dual-energy. In this example orange represents organic materials, and blue metals. The intensity of this image corresponds to the thickness of the materials (courtesy by M. Baştan [3]).

and isolated from the background of the scene. Significant features of the segmented parts are extracted. Selected features are classified or analyzed in order to determine if the test object deviates from a given set of specifications. Using a supervised pattern recognition methodology, the selection of the features and the training of the classifier are performed using representative images that are to be labeled by experts [9].

For the segmentation task, two general approaches can be used: a traditional image segmentation or a *sliding-window* approach. In the first case, image processing algorithms are used (*e.g.* histograms, edge detection, morphological operations, filtering, etc. [13]). Nevertheless, inherent limitations of traditional segmentation algorithms for complex tasks and increasing computational power have fostered the emergence of an alternative approach based on the so-called *sliding-window* paradigm. Sliding-window approaches have established themselves as state-of-art in computer vision problems where a visually complex object must be separated from the background (see, for example, successful applications in face detection [51] and human detection [6]). In the sliding-window approach, a detection window is moved over an input image in both horizontal and vertical directions, and for each localization of the detection window, a classifier decides to which class the corresponding portion of the image belongs according to its features. Here, a set of candidate image areas are selected and all of them are fed to the subsequent parts of the image analysis algorithm. This resembles a brute force approach where the algorithm explores a large set of possible segmentations, and at the end the most suitable is selected by the classification steps. An example for weld inspection using sliding-windows can be found in [32].

2.3. Geometric model

The X-ray image of a test object corresponds to a projection in perspective, where a 3D point of the test object is viewed as a pixel in the digital X-ray image, as illustrated in Fig. 1. A geometric model that describes this projection can be highly useful for 3D reconstruction and for data association between different views of the same object. Thus, 3D features or multiple view 2D features can be used to improve the diagnosis performed by using a single view.

For the geometric model, four coordinate systems are used (see Fig. 1):

- OCS (X, Y, Z) : Object Coordinate System, where a 3D point is defined using coordinates attached to the test object.
- WCS $(\bar{X}, \bar{Y}, \bar{Z})$: World Coordinate System, where the origin corresponds to the optical center (X-ray source) and the \bar{Z} axis is perpendicular to the projection plane of the detector.
- PCS (x, y) : Projection Coordinate System, where the 3D point is projected into the projection plane $\bar{Z} = f$, and the origin is the intersection of this plane with \bar{Z} axis.
- ICS (u, v) : Image Coordinate System, where a projected point is viewed in the image. In this case, (x, y) -axes are set to be parallel to (u, v) -axes.

The geometric model $\text{OCS} \rightarrow \text{ICS}$, *i.e.* transformation $\mathbf{P} : (X, Y, Z) \rightarrow (u, v)$, can be expressed in homogeneous coordinates as [28]:

$$\lambda \begin{bmatrix} u \\ v \\ 1 \end{bmatrix} = \mathbf{P} \begin{bmatrix} X \\ Y \\ Z \\ 1 \end{bmatrix}, \quad (3)$$

where λ is a scale factor and \mathbf{P} is a 3×4 matrix modeled as three transformations:

- i*) $\text{OCS} \rightarrow \text{WCS}$, *i.e.* transformation $\mathbf{T}_1 : (X, Y, Z) \rightarrow (\bar{X}, \bar{Y}, \bar{Z})$, using a 3D rotation matrix \mathbf{R} , and 3D translation vector \mathbf{t} ;
- ii*) $\text{WCS} \rightarrow (\text{PCS})$, *i.e.* transformation $\mathbf{T}_2 : (\bar{X}, \bar{Y}, \bar{Z}) \rightarrow (x, y)$, using a perspective projection matrix that depends on focal distance f ; and
- iii*) $\text{PCS} \rightarrow \text{ICS}$, *i.e.* transformation $\mathbf{T}_3 : (x, y) \rightarrow (u, v)$, using scales factor α_x and α_y , and 2D translation vector (u_0, v_0) .

The three transformations $\text{OCS} \rightarrow \text{WCS} \rightarrow \text{PCS} \rightarrow \text{ICS}$ are expressed as:

$$\mathbf{P} = \underbrace{\begin{bmatrix} \alpha_x & 0 & u_0 \\ 0 & \alpha_x & v_0 \\ 0 & 0 & 1 \end{bmatrix}}_{\mathbf{T}_3} \underbrace{\begin{bmatrix} f & 0 & 0 & 0 \\ 0 & f & 0 & 0 \\ 0 & 0 & 1 & 0 \end{bmatrix}}_{\mathbf{T}_2} \underbrace{\begin{bmatrix} \mathbf{R} & \mathbf{t} \\ \mathbf{0}^\top & 1 \end{bmatrix}}_{\mathbf{T}_1} \quad (4)$$

The parameters included in matrix \mathbf{P} can be estimated using a calibration approach [16].

In order to obtain multiple views of the object, m different projections of the test object can be achieved by rotating and translating it (for this task a manipulator can be used). For the k -th projection, for $k = 1 \dots m$, the geometric model \mathbf{P}_k used in (3) is computed from (4) including 3D rotation matrix \mathbf{R}_k and 3D translation \mathbf{t}_k . Matrices \mathbf{P}_k can be estimated using a calibration object projected in the m different positions [28] or using a bundle adjustment algorithm where the geometric model is obtained from the m X-ray images of the test object [31].

2.4. Multiple view analysis

It is well known that *an image says more than thousand words*, however, this is not always true if we have an *intricate* image. In certain X-ray applications, *e.g.* baggage inspection, there are usually *intricate* X-ray images due to overlapping parts inside the test object, where each pixel corresponds to the attenuation of multiple parts, as expressed in (2).

In some cases, *active vision* can be used in order to adequate the viewpoint of the test object to obtain more suitable X-ray images to analyze. Therefore, an algorithm is designed for guiding the manipulator of the X-ray imaging system to poses where the detection performance should be higher [42] (see Fig. 1).

In other cases, multiple view analysis can be a powerful option for examining complex objects where uncertainty can lead to misinterpretation. Multiple view analysis offers advantages not only in 3D interpretation. Two or more images of the same object taken from different points of view can be used to confirm and improve the diagnosis undertaken by analyzing only one image.

Multiple view analysis in X-ray testing can be used to achieve two main goals: *i*) analysis of 2D corresponding features across the multiple views, and *ii*) analysis of 3D features obtained from a 3D reconstruction approach. In both cases, the attempt is made to gain relevant information about the test object. For instance, in order to validate a single view detection –filtering out false alarms– 2D corresponding features can be analyzed [33]. On the other hand, if the geometric dimension of a inner part must be measured a 3D reconstruction needs to be performed [38].

As illustrated in Fig. 1, the input of the multiple view analysis is the *associated data*, *i.e.* corresponding points (or patches) across the multiple views. To this end, associated 2D cues are found using geometric constraints (*e.g.* epipolar geometry and multifocal tensors [16, 29]), and local scale-invariant descriptors across multiple views (*e.g.* like SIFT [25]).

Finally, 2D or 3D features of the associated data can be extracted and selected, and a classifier can be trained using the same pattern recognition methodology explained in Section 2.2.

Table 1. Applications on X-ray testing

Appli- cation	First author	Year	Refe- rence	Energy		Geometric Model ^(*)	Single Views ^(**)			Active Vision	Multiple Views ^(**)		
				Mono	Dual		①	②	③		①	②	③
Casting	Carrasco	2011	[4]	×		N	×	×	×		×	×	×
	Li	2006	[22]	×		–	×	×					
	Mery	2002	[33]	×		C	×	×	×		×	×	×
	Pieringer	2010	[40]	×		C	×	×	×		×	×	×
	Tang	2009	[50]	×		–	×						
Weld	Liao	2008	[23]	×		–	×	×	×				
	Liao	2009	[24]	×		–	×	×	×				
	Mery	2011	[32]	×		–	×	×	×				
	Shi	2007	[45]	×		–	×						
Baggage	Abusaceda	2011	[1]	×	×	C	×						
	Baştan	2012	[3]	×	×	–	×	×	×				
	Chen	2005	[5]	×	×	–	×						
	Ding	2006	[7]	×	×	–	×						
	Franzel	2012	[10]	×	×	C	×	×	×		×	×	×
	Heitz	2010	[17]	×	×	–	×	×	×				
	Mansoor	2012	[27]	×	×	–	×	×	×				
	Mery	2013	[35]	×		N	×	×	×		×	×	×
	Qiang	2006	[26]	×	×	–	×	×					
	Rahman	2010	[41]	×	×	–	×						
	Riffo	2011	[42]	×		N	×	×		×			
	Schmidt	2012	[44]	×	×	–	×	×	×				
	Singh	2005	[48]	×	×	–	×						
Food	Haff	2004	[14]	×		–	×	×	×				
	Jiang	2008	[20]	×		–	×	×	×				
	Ogawa	2003	[39]	×		–	×	×	×				
	Kwon	2008	[21]	×		–	×	×	×				
	Mery	2011	[34]	×		–	×	×	×				
Cargo	Duan	2008	[8]	×		–	×	×	×				
	Frosio	2011	[11]	×		–	×	×	×	×			
	Zhu	2008	[55]	×		–	×	×	×				

(*) C: Calibrated, N: Not calibrated, –: not used.

(**) See ①, ②, ③ in Fig. 1

Depending on the application, the output could be a measurement (e.g. the volume of the inspected inner part is 3.4cm³), a class (e.g. the test object is defective) or an interpretation (e.g. the baggage should be inspected by a human operator given that uncertainty is high).

3. Applications

In this Section, the state-of-the-art of certain relevant applications on X-ray testing will be described. This section covers X-ray testing in *i*) casting, *ii*) weld, *iii*) baggage, *iv*) food, and *v*) cargo. In Table 1, approaches in each application are summarized showing how they use the different steps of general diagram according to Fig. 1.

3.1. Casting

Light-alloy castings produced for the automotive industry, such as wheel rims, steering knuckles and steering gear boxes are considered important components for overall roadworthiness. Non-homogeneous regions can be formed within the work piece in the production process. These are manifested, for example, by bubble-shaped voids, fractures, inclusions or slag formation. To ensure the safety of a construction, it is necessary to check every part thoroughly using X-ray testing. In casting inspection, automated X-ray systems have not only raised quality, through repeated objective inspections and improved processes, but have also increased productivity and consistency by reducing labor

costs. A survey can be found in [30]. Selected approaches are summarized in Table 1. In this area, we conclude that automated systems are very effective, as the inspection task is fast and achieves a high performance.

3.2. Weld

In welding process, a mandatory inspection using X-ray testing is required in order to detect defects such as porosity, inclusion, lack of fusion, lack of penetration and cracks. Industrial X-ray images of welds are commonly used to detect defects in the petroleum, chemical, nuclear, naval, aeronautics and civil construction industries, among others. A survey can be found in [46, 47]. Selected approaches are summarized in Table 1. As we can see, there is much research on weld inspection. However, achieved performance of the developed algorithms is still not high enough, making it unsuitable for fully automated inspection.

3.3. Baggage

Since 11/9, automated (or semi-automated) 3D recognition using X-ray images has become a very important issue in baggage screening [54, 37]. The inspection process is highly complex as hazardous items are very difficult to detect when placed in close packed bags, superimposed by other objects, and/or rotated showing an unrecognizable profile. During the last decade, however, relevant research has been carried out in multiple view analysis and dual-energy imaging. The use of multiple view information yields a significant improvement in performance, as certain items are difficult to recognize using only one viewpoint [52]. On the other hand, when dual-energy is employed it is possible to identify the material composition –typically for explosives, drugs and organic materials– [49]. A survey on explosive detection can be found in [49, 53]. Selected approaches are summarized in Table 1. We conclude, that in baggage screening, where human security plays an important role and inspection complexity is very high, human inspectors are still used. For intricate conditions, multiple view X-ray inspection using dual-energy is required.

3.4. Food

In order to ensure food safety inspection, several applications have been developed by the food industry. The difficulties inherent in the detection of defects and contaminants in food products have limited the use of X-ray in the packaged foods sector. However, the need for NDT has driven a considerable research effort in this field over various decades [15]. The most important advances are: detection of foreign objects in packaged foods [21]; detection of fish bones in processed fish [34]; identification of insect infestation in citrus fruit [20]; detection of codling moth larvae in apples [15]; fruit quality inspection such as split-pits, water content distribution and internal structure [39]; and

detection of larval stages of the granary weevil in wheat kernels [14]. In these applications, only single view analysis is required. A survey can be found in [15]. In Table 1, the mentioned applications are summarized.

3.5. Cargo

With the ongoing development of international trade, cargo inspection becomes more and more important. X-ray testing has been used for the evaluation of the contents of cargo, trucks, containers, and passenger vehicles to detect the possible presence of many types of contraband. Some approaches are presented in Table 1. However, limited research has been undertaken on cargo inspection, and the complexity of this inspection task is very high. For this reason, we conclude that these X-ray systems continue to be only semi-automatic, and require human supervision.

4. Data Bases

Public databases of X-ray images can be found for medical imaging³, however, to the best knowledge of the author of this article, up until now there have not been any public databases of digital X-ray images for X-ray testing.

As a service to the X-ray testing community, we collected more than 3000 X-ray images for the development, testing and evaluation of image analysis and computer vision algorithms. The images are organized in a public database referred to as GDXray: The GRIMA X-ray database⁴. The database includes three groups of X-ray images: metal objects (castings, welds, razor blades, ninja stars (*shuriken*), guns, knives and sink strainers), baggage (bags and pen cases); and natural objects (fruits, fish bones and wood).

5. Conclusions

In this paper we presented a general overview of computer vision methodologies that have been used in X-ray testing, as illustrated in diagram of Fig. 1. The presented applications on X-ray testing follow this general schema, where depending on the way the X-ray images are acquired and analyzed, each step can be (or not be) used.

In the presented applications, we observed that there are some areas, such as casting inspections, where automated systems are very effective; and other application areas, like baggage screening, where human inspection is still used.

³See for example a good collection in <http://www.via.cornell.edu/databases/>

⁴GRIMA is the name of our Machine Intelligence Group at the Department of Computer Science of the Pontificia Universidad Católica de Chile <http://grima.ing.puc.cl>. The X-ray images included in GDXray can be used free of charge, but for research and educational purposes only. Redistribution and commercial use is prohibited. Any researcher reporting results which use this database should acknowledge the GDXray database by citing [36].

Additionally, there are certain application areas, including weld and cargo inspection, where the inspection is semi-automatic. Finally, some food analysis research is beginning to be characterized by the use of X-ray imaging.

It is clear that many research directions have been exploited, some very different principles have been adopted and a wide variety of algorithms have been developed for very different applications. Nevertheless, automated X-ray testing remains an open interrogation as it still suffers from: i) *loss of generality* given that approaches developed for one application may not be used in another; ii) *deficient detection accuracy* as commonly there is a fundamental trade-off between false alarms and misdetections; iii) *limited robustness* because prerequisites for the use of a method are often fulfilled only in simple cases; and iv) *low adaptability* as it may be very difficult to accommodate an automated system to design modifications or different objects.

Compared to manual X-ray testing, automated systems offer advantages of objectivity and reproducibility for every test. Fundamental disadvantages are, however, the complexity of their configuration, the inflexibility to any change in the evaluation process, and sometimes the inability to analyze intricate images, which is something that people can generally do well. Research and development is, however, ongoing into automated adaptive processes to accommodate modifications.

Acknowledgments

This work was supported by Fondecyt grant 1130934 awarded by CONICYT-Chile. The author wishes to thank M. Baştan from the Image Understanding and Pattern Recognition Group, at the Technical University of Kaiserslautern, Germany, for sharing Fig. 2.

References

- [1] O. Abusaeeda, J. Evans, D. D., and J. Chan. View synthesis of KDEX imagery for 3D security X-ray imaging. In *Proc. 4th International Conference on Imaging for Crime Detection and Prevention (ICDP-2011)*, 2011.
- [2] J. Als-Neielsen and D. McMorrow. *Elements of modern X-ray physics*. Willey, second edition, 2011.
- [3] M. Baştan, M. R. Yousefi, and T. M. Breuel. Visual words on baggage X-ray images. In *Computer Analysis of Images and Patterns*, pages 360–368. Springer, 2011.
- [4] M. Carrasco and D. Mery. Automatic multiple view inspection using geometrical tracking and feature analysis in aluminum wheels. *Machine Vision and Applications*, 22(1):157–170, 2011.
- [5] Z. Chen, Y. Zheng, B. R. Abidi, D. L. Page, and M. A. Abidi. A combinational approach to the fusion, de-noising and enhancement of dual-energy x-ray luggage images. In *IEEE Conference on Computer Vision and Pattern Recognition (CVPR-2005), Workshop CDROM*, 2005.
- [6] N. Dalal and B. Triggs. Histograms of oriented gradients for human detection. In *European Conference on Computer Vision (ECCV)*, 2005.
- [7] J. Ding, Y. Li, X. Xu, and L. Wang. X-ray image segmentation by attribute relational graph matching. In *8th IEEE International Conference on Signal Processing*, volume 2, 2006.
- [8] X. Duan, J. Cheng, L. Zhang, Y. Xing, Z. Chen, and Z. Zhao. X-ray cargo container inspection system with few-view projection imaging. *Nuclear Instruments and Methods in Physics Research A*, 598:439–444, 2009.
- [9] R. Duda, P. Hart, and D. Stork. *Pattern Classification*. John Wiley & Sons, Inc., New York, 2 edition, 2001.
- [10] T. Franzel, U. Schmidt, and S. Roth. Object detection in multi-view X-ray images. *Pattern Recognition*, pages 144–154, 2012.
- [11] I. Frosio, N. Borghese, F. Lissandrello, G. Venturino, and G. Rotondo. Optimized acquisition geometry for X-ray inspection. In *Instrumentation and Measurement Technology Conference (I2MTC), 2011 IEEE*, pages 1–6, 2011.
- [12] J. Goebbels. *Handbook of Technical Diagnostics*, chapter Computed Tomography, pages 249–258. Springer, 2013.
- [13] R. Gonzalez and R. Woods. *Digital Image Processing, 2nd ed.* Addison-Wesley, third edition, 2007.
- [14] R. Haff and D. Slaughter. Real-time X-ray inspection of wheat for infestation by the granary weevil, *sitophilus granarius* (L.). *Transactions of the American Society of Agricultural Engineers*, 47:531–537, 2004.
- [15] R. P. Haff and N. Toyofuku. X-ray detection of defects and contaminants in the food industry. *Sensing and Instrumentation for Food Quality and Safety*, 2(4):262–273, 2008.
- [16] R. I. Hartley and A. Zisserman. *Multiple view geometry in computer vision*. Cambridge University Press, second edition, 2003.
- [17] G. Heitz and G. Chechik. Object separation in X-ray image sets. In *IEEE Conference on Computer Vision and Pattern Recognition (CVPR-2010)*, pages 2093–2100, 2010.
- [18] C. Hellier. *Handbook of Nondestructive Evaluation*. McGraw Hill, second edition, 2013.
- [19] J. Hubbell and S. Seltzer. Tables of X-Ray mass attenuation coefficients and mass energy-absorption coefficients from 1 keV to 20 MeV for elements Z = 1 to 92 and 48 additional substances of dosimetric interest. <http://www.nist.gov/pml/data/xraycoef/index.cfm>, 1996.
- [20] J.-A. Jiang, H.-Y. Chang, K.-H. Wu, C.-S. Ouyang, M.-M. Yang, E.-C. Yang, T.-W. Chen, and T.-T. L. a. An adaptive image segmentation algorithm for x-ray quarantine inspection of selected fruits. *Computers and Electronics in Agriculture*, 60:190–200, 2008.
- [21] J.-S. Kwon, J.-M. Lee, and W.-Y. Kim. Real-time detection of foreign objects using x-ray imaging for dry food manufacturing line. In *Proceedings of IEEE International Symposium on Consumer Electronics (ISCE 2008)*, pages 1–4, April 2008.
- [22] X. Li, S. K. Tso, , X.-P. Guan, and Q. Huang. Improving automatic detection of defects in castings by applying wavelet technique. *IEEE Transactions on Industrial Electronics*, 53(6):1927–1934, 2006.

- [23] T. Liao. Classification of weld flaws with imbalanced class data. *Expert Systems with Applications*, 35(3):1041–1052, 2008.
- [24] T. W. Liao. Improving the accuracy of computer-aided radiographic weld inspection by feature selection. *NDT&E International*, 42:229239, 2009.
- [25] D. Lowe. Distinctive image features from scale-invariant keypoints. *International Journal of Computer Vision*, 60(2):91–110, 2004.
- [26] Q. Lu and R. Conners. Using image processing methods to improve the explosive detection accuracy. *IEEE Transactions on Applications and Reviews, Part C: Systems, Man, and Cybernetics*, 36(6):750–760, 2006.
- [27] M. Mansoor and R. Rajashankari. Detection of concealed weapons in X-ray images using fuzzy K-NN. *International Journal of Computer Science, Engineering and Information Technology*, 2(2), 2012.
- [28] D. Mery. Explicit geometric model of a radiosopic imaging system. *NDT & E International*, 36(8):587–599, 2003.
- [29] D. Mery. Exploiting multiple view geometry in X-ray testing: Part I, theory. *Materials Evaluation*, 61(11):1226–1233, November 2003.
- [30] D. Mery. Automated radiosopic testing of aluminum die castings. *Materials Evaluation*, 64(2):135–143, 2006.
- [31] D. Mery. Automated detection in complex objects using a tracking algorithm in multiple X-ray views. In *Proceedings of the 8th IEEE Workshop on Object Tracking and Classification Beyond the Visible Spectrum (OTCBVS 2011), in Conjunction with CVPR 2011, Colorado Springs*, pages 41–48, 2011.
- [32] D. Mery. Automated detection of welding discontinuities without segmentation. *Materials Evaluation*, (June):657–663, 2011.
- [33] D. Mery and D. Filbert. Automated flaw detection in aluminum castings based on the tracking of potential defects in a radiosopic image sequence. *IEEE Trans. Robotics and Automation*, 18(6):890–901, December 2002.
- [34] D. Mery, I. Lillo, V. Riffo, A. Soto, A. Cipriano, and J. Aguilera. Automated fish bone detection using X-ray testing. *Journal of Food Engineering*, 2011(105):485–492, 2011.
- [35] D. Mery, G. Mondragón, V. Riffo, , and I. Zuccar. Detection of regular objects in baggage using multiple x-ray views. *Insight*, 55(1):16–20, 2013.
- [36] D. Mery, U. Zscherpel, V. Riffo, G. Mondragón, I. Lillo, I. Zuccar, and H. Löbel. GDXray – the GRIMA database of X-ray images. <http://dmery.ing.puc.cl/index.php/material/gdxray/>. Department of Computer Science, Universidad Católica de Chile.
- [37] S. Michel, S. Koller, J. de Ruiter, R. Moerland, M. Hogervorst, and A. Schwaninger. Computer-based training increases efficiency in X-Ray image interpretation by aviation security screeners. pages 201–206, Oct. 2007.
- [38] A. Noble, R. Gupta, J. Mundy, A. Schmitz, and R. Hartley. High precision X-ray stereo for automated 3D CAD-based inspection. *IEEE Trans. Robotics and Automation*, 14(2):292–302, 1998.
- [39] Y. Ogawa, N. Kondo, and S. Shibusawa. Inside quality evaluation of fruit by x-ray image. volume 2, pages 1360–1365 vol.2, July 2003.
- [40] C. Pieringer and D. Mery. Flaw detection in aluminium die castings using simultaneous combination of multiple views. *Insight*, 52(10):548–552, 2010.
- [41] S. M. Rahman, M. O. Ahmad, and M. Swamy. Contrast-based fusion of noisy images using discrete wavelet transform. *Image Processing, IET*, 4(5):374–384, 2010.
- [42] V. Riffo and D. Mery. Active X-ray testing of complex objects. *Insight*, 54(1):28–35, 2012.
- [43] J. Rowlands. The physics of computed radiography. *Physics in medicine and biology*, 47(23):R123, 2002.
- [44] L. Schmidt-Hackenberg, M. R. Yousefi, and T. M. Breuel. Visual cortex inspired features for object detection in X-ray images. In *Pattern Recognition (ICPR), 2012 21st International Conference on*, pages 2573–2576. IEEE, 2012.
- [45] D.-H. Shi, T. Gang, S.-Y. Yang, and Y. Yuan. Research on segmentation and distribution features of small defects in precision weldments with complex structure. *NDT & E International*, 40:397–404, 2007.
- [46] R. Silva and D. Mery. State-of-the-art of weld seam inspection using X-ray testing: Part i image processing. *Materials Evaluation*, 65(6):643–647, 2007.
- [47] R. Silva and D. Mery. State-of-the-art of weld seam inspection using X-ray testing: Part ii pattern recognition. *Materials Evaluation*, 65(9):833–838, 2007.
- [48] M. Singh and S. Singh. Optimizing image enhancement for screening luggage at airports. In *Computational Intelligence for Homeland Security and Personal Safety, 2005. CIHSPS 2005. Proceedings of the 2005 IEEE International Conference on*, pages 131–136, 31 2005-april 1 2005.
- [49] S. Singh and M. Singh. Explosives detection systems (eds) for aviation security. *Signal Processing*, 83(1):31–55, 2003.
- [50] Y. Tang, X. Zhang, X. Li, and X. Guan. Application of a new image segmentation method to detection of defects in castings. *The International Journal of Advanced Manufacturing Technology*, 43(5-6):431–439, 2009.
- [51] P. Viola and M. Jones. Robust real-time object detection. *International Journal of Computer Vision*, 57(2):137–154, 2004.
- [52] C. von Bastian, A. Schwaninger, and S. Michel. *Do Multi-view X-ray Systems Improve X-ray Image Interpretation in Airport Security Screening?*, volume 52. GRIN Verlag, 2010.
- [53] K. Wells and D. Bradley. A review of X-ray explosives detection techniques for checked baggage. *Applied Radiation and Isotopes*, 2012.
- [54] G. Zentai. X-ray imaging for homeland security. *Imaging Systems and Techniques, 2008. IST 2008. IEEE International Workshop on*, pages 1–6, Sept. 2008.
- [55] Z. Zhu, L. Zhao, and J. Lei. 3d measurements in cargo inspection with a gamma-ray linear pushbroom stereo system. In *Proceedings of the 2005 IEEE Computer Society Conference on Computer Vision and Pattern Recognition (CVPR05)*, 2005.